REVIEW OF INSTABILITIES WITH IONS OR/AND ELECTRONS AND POSSIBLE MITIGATIONS

L. Mether*, CERN, Geneva, Switzerland

Abstract

The presence of ions and electrons from gas ionization, photoemission or secondary emission is unavoidable in the vacuum chambers of high intensity accelerators and storage rings. Under suitable conditions, these ions and electrons can accumulate and drive the beams unstable. In this contribution, the mechanisms behind and the main conditions for ion and electron accumulation in the bunched beams are summarized. The characteristics of the induced instabilities, as well as common modelling techniques and mitigation strategies are reviewed. The possible interplays between ions and electrons are also discussed.

INTRODUCTION

Electromagnetic fields in the beam environment, in addition to the externally applied RF and magnetic fields, may perturb the motion of the beam particles and give rise to instabilities. Whereas impedance and space charge are caused by electromagnetic fields induced by the beam itself, electron and ion instabilities are two-stream instabilities that are caused by the presence of another set of charged particles. Typically, this other set of particles is generated by the beam itself directly or indirectly. Electrons and ions are produced through, for example, the beam-induced ionization of residual gas in the beam chamber, photoemission from synchrotron radiation and outgassing due to particles impacting the beam chamber. Particles with the same sign of electrical charge as the beam particles are repelled by the beam and therefore rarely accumulate, whereas particles with the opposite sign of electrical charge, which are attracted by the beam field, are prone to accumulation. Consequently ion accumulation is typically observed in electron machines and electron cloud build-up in positron and proton machines.

ION INSTABILITIES

Beam-induced gas ionization gives rise to electrons and ions along the beam path. In electron machines, positive ions are attracted by the negative beam field and may become trapped in the beam potential and oscillate around the bunch train, as illustrated in Fig. 1a. Classical ion instabilities, where ions are trapped and accumulate over several turns in a synchrotron, can be avoided with a sufficiently long clearing gap in the bunch train pattern. In the presence of a clearing gap, ions can only accumulate over a single turn, but can still give rise to a fast beam-ion instability [1,2]. Fast beam-ion instabilities can occur also in linear accelerators.

Due to their relatively large mass, ions typically do not move sufficiently during the passage of individual bunches to cause head-tail instabilities. Instead, the ions transfer information on the offset of their generating bunch to the following bunches and thus may lead to coupled-bunch instabilities. The instabilities are typically accompanied by transverse emittance growth and a coherent tune shift. In particular for the fast beam-ion instability, the effects are usually stronger at the tail of the bunch trains, since the density of trapped ions increases along the trains.

Classical ion instabilities have been observed in several machines since the 60's [3]. Fast beam-ion instabilities have also been observed in many machines since they were first predicted in the 90's [4]. In most cases, fast beam-ion instabilities have been observed in the presence of vacuum degradation e.g. during commissioning, due to a local pressure rise such as from impedance heating, or during dedicated experiments with additional injected gas.

The fast beam-ion instability can be analytically modelled using the linear approximation of a two-dimensional Gaussian beam field [1]. In this approximation, an ion with mass number A at the transverse position (x, y) receives the following velocity kick by the beam

$$\frac{2N_b r_p c}{A} \frac{x, y}{\left(\sigma_x + \sigma_y\right) \sigma_{x,y}} \equiv k_{x,y} * x, y \,, \tag{1}$$

where N_b is the bunch intensity, r_p the classical proton radius, c the speed of light and $\sigma_{x,y}$ are the transverse beam sizes. During the bunch spacing T_b the ions drift. By analogy with the stability condition of a linear beam trajectory, $|\mathrm{Tr}(M)| < 2$, the motion is stable if $k_{x,y} T_b < 4$. This leads to a lower limit on the ion mass number for trapping to occur

$$A > A_{\mathrm{trap}} = \frac{N_b r_p T_b c}{2\left(\sigma_x + \sigma_y\right) \sigma_{x,y}} \,. \tag{2}$$

Neglecting the presence of a spread in the oscillation frequency of the trapped ions, the instability rise time can be estimated as

$$\tau_{\mathrm{inst}}^2 \propto \frac{\gamma^2 A \omega_\beta}{n_b^4 N_b^3 P^2 T_b c} \left(\sigma_x + \sigma_y\right)^3 \sigma_{x,y}^3 \,. \tag{3}$$

Here γ is the Lorentz factor of the beam, n_b is the number of bunches in the train, ω_β is the (angular) betatron frequency and P is the partial vacuum pressure for the species considered.

However, the linear approximation is accurate only for ions oscillating within a small region around the centre of the beam, with $x, y \lesssim \sigma_{x,y}$. This condition is more easily satisfied for heavier ions with mass numbers that are well above the trapping mass number A_{trap}. In the non-linear regime, ion trajectories are significantly altered with respect

* lotta.mether@cern.ch

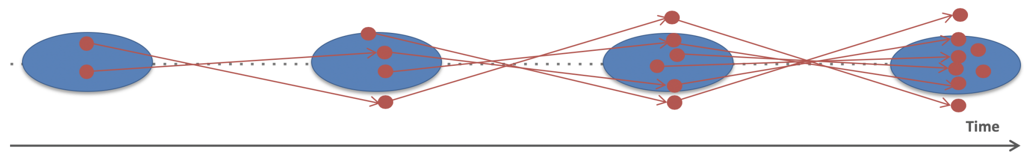

(a) Ion accumulation along an electron bunch train.

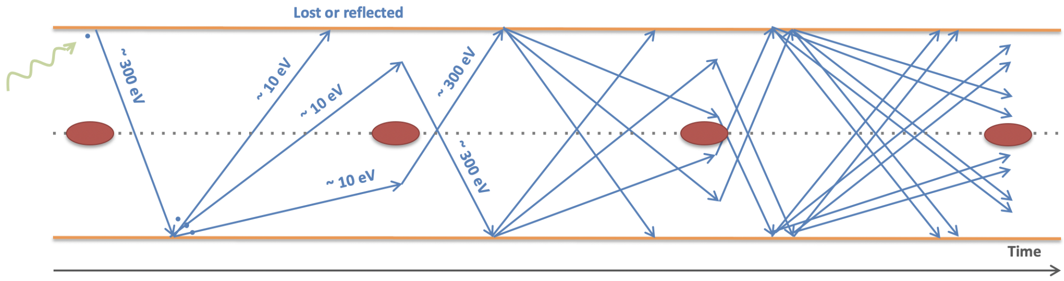

(b) Electron cloud build-up along a proton/positron bunch train.

Figure 1: Schematic diagrams of ion accumulation in electron machines (a) and electron cloud build-up in positron or proton machines (b).

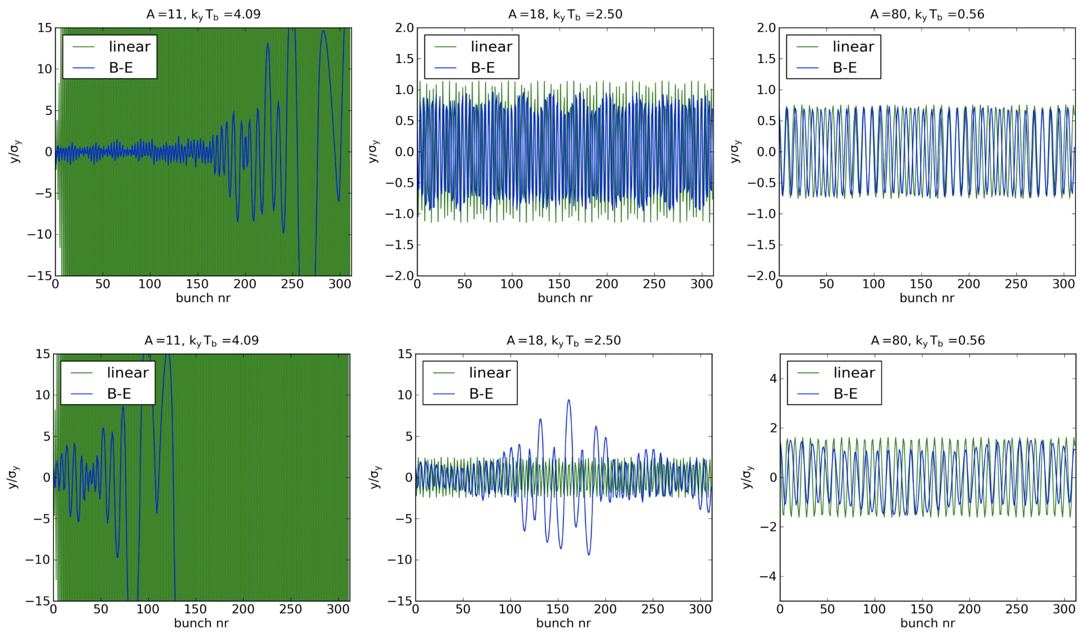

Figure 2: Comparison of ion trajectories along a bunch train using the linear approximation and the Bassetti-Erskine formula [5] for the beam field for different ion mass numbers (left to right). The top and bottom rows show trajectories with initial amplitudes of 0.7 σ and 1.5 σ respectively.

to the linear approximation and the trapping condition Eq. (2) is not strictly valid, as shown in Fig. 2. As illustrated in the left column of the figure, the non-linearity of the beam field alters the ion trapping such that ions that would be over-focused and lost in the linear regime are in fact trapped in an oscillation around the beam for a significant amount of time. The non-linear beam field also introduces a spread in the ion oscillation frequency. Extensions of the theory to the non-linear regime suggest that the non-linearity damps the instability, such that the growth rate becomes linear rather than exponential [6].

The full beam-ion interaction, including non-linearities, can be accurately modelled using macro-particle simulations. The simulations can be done in the strong-strong regime, where both the beam and ions are represented by macro-particles, or the weak-strong regime, where only the ions are modelled with macro-particles. The strong-strong simulations, in particular, are typically computationally very heavy, but they have the benefit of being able to model also the evolution of the beam emittance. Instabilities caused by ion trapping in the non-linear regime were observed in a recent simulation study [7]. Compared to the standard fast beam-ion instability, these instabilities showed atypical characteristics, e.g. the instability developed simultaneously over most of the train rather than developing from the tail of the train towards the head and the instability was stronger for larger ion mass numbers contrary to the prediction of Eq. (3).

Apart from the non-linearity of the beam field, the variation of the beta functions along the machine and the presence of multiple gas species can also have a damping effect on the instability. In addition, the instability also strongly depends on the filling pattern. All of these effects can readily be taken into account in macro-particle simulations. Fast beam-ion instabilities have also successfully been modelled using a wake field formalism [8,9], which allows taking into account several of these effects.

ELECTRON INSTABILITIES

Electrons are produced in the beam chamber e.g. through beam-induced gas ionization and photoemission from synchrotron radiation. Such seed electrons are accelerated by the beam and can induce secondary electron emission from the chamber wall on their impact. With a positively charged beam, a subsequent bunch will accelerate these secondary electrons across the chamber and, as they hit the wall, further secondary emission can be induced. In this way, as illustrated in Fig. 1b, secondary electron emission can lead to avalanche electron multiplication through beam-induced multipacting over several bunch passages, until a dynamical equilibrium is reached.

The conditions for electron cloud build-up depend on several parameters including the bunch spacing, the chamber geometry, external magnetic fields, the bunch charge and length, as well as the secondary emission yield (SEY) of the chamber surface. The SEY is defined as the ratio between the emitted and impacting electron currents and is a function of the energy and angle of incidence of the impacting electrons. The SEY of a given surface depends on its chemical and physical properties, which may change over time.

Whereas ions barely move during the passage of individual bunches, the much lighter electrons move significantly during a single bunch passage. Electrons attracted by the beam field are pulled into the bunch (the so-called pinch) and oscillate in the beam field during the bunch passage. This gives rise to a z-dependent electron density along the bunch, which can induce coupling between the head and the tail of the bunch and eventually drive the bunch unstable. As a consequence of the electron motion within the bunch, fast intra-bunch motion is characteristic for single bunch electron cloud instabilities. The instabilities are often accompanied by beam losses and transverse emittance growth.

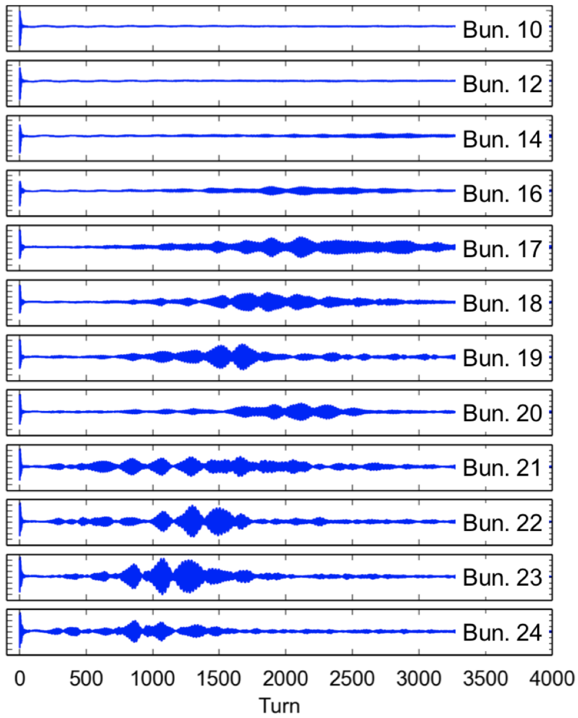

(a) Single-bunch (vertical) instabilities in the LHC [10].

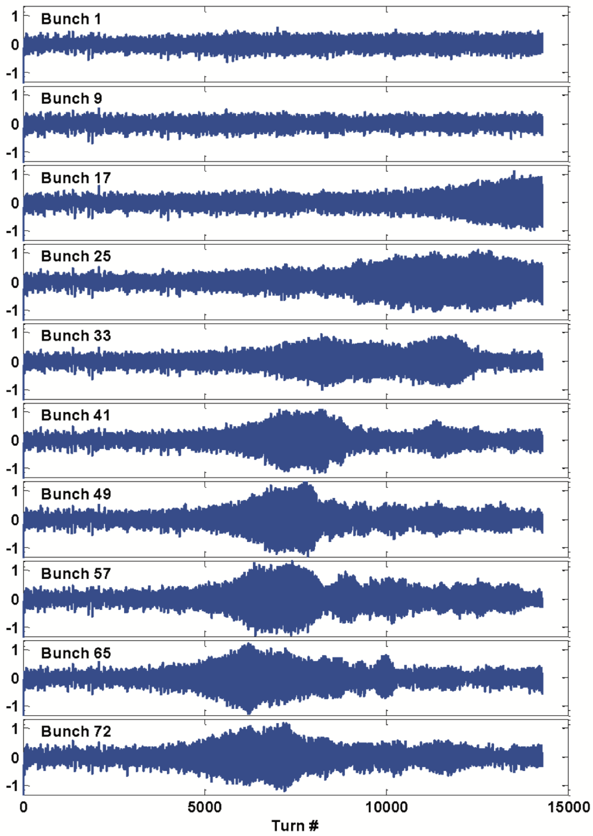

(b) Coupled-bunch (horizontal) instability in the PS [11].

Figure 3: Measured centroid positions for selected bunches along bunch trains suffering from single- and coupled-bunch electron cloud instabilities in CERN accelerators.

Since the electron cloud survives on the time scale of several bunch passages, it can also be responsible for bunch-to-bunch coupling and coupled-bunch instabilities. These instabilities are likely to occur in situations where the electron motion is constrained, such that a memory of the electron distribution is maintained from one bunch to the following. This can be the case e.g. in the presence of externally applied magnetic fields such as dipole fields. Since electron clouds build up along the bunch trains, bunches at the tail of trains encounter a larger electron density than bunches at the head of trains and are therefore most affected by both single- and coupled-bunch instabilities. This is illustrated by the transverse position measurements shown in Fig. 3.

Electron cloud instabilities were first observed in the 60's. Since then, electron cloud has been observed in several different machines, through many related effects [10,12]. Apart from instabilities, electron cloud effects on the beam dynamics include tune shifts along the bunch train and incoherent effects such as tune spread and emittance growth, which may lead to slow beam losses. An RF stable phase shift is induced as a consequence of the beam energy lost to the electrons [13]. Electron clouds can also affect the vacuum quality, through outgassing leading to a pressure rise. Finally, the impinging electrons deposit a heat load on the chamber walls, which can be problematic in particular in superconducting machines. Currently electron cloud effects are present during operation e.g. in the LHC [14] and at SuperKEKB [15].

Analytical models have been developed to study the behaviour of electrons in the beam potential and the induced instabilities. The electron oscillations in the beam field during the pinch can be modelled similarly to the ion motion in the electron beam in Eq. (1). As shown in Fig. 4, within the validity regime of the linear approximation, i.e. for an electron with an oscillation amplitude that is smaller than the rms beam size, there is good agreement between the linear analytical theory and simulations [16]. Models using a wake field formalism have been developed for studying the resulting head-tail instability, although the electron cloud cannot be considered a time-invariant system due to the electron motion during the bunch passage [17–19].

Due to the complexity of the electron cloud build-up and instability processes, a comprehensive understanding of electron cloud effects currently relies on macro-particle simulations. For single-bunch electron cloud instabilities the problem can be divided into two parts: electron cloud build-up simulations with a rigid beam and subsequent beam dynamics simulations of the instability, where electron distributions saved in build-up simulations can be used to initialize the electrons [20]. For coupled-bunch instabilities, on the other hand, the build-up must be performed dynamically over the full bunch train to capture the instability mechanism [21]. However, several aspects of coupled-bunch instabilities have successfully been modelled analytically with wake field models [22–24], similarly to the fast beam ion instability.

Full scale electron cloud instability simulations are demanding both in terms of computing resources and time.

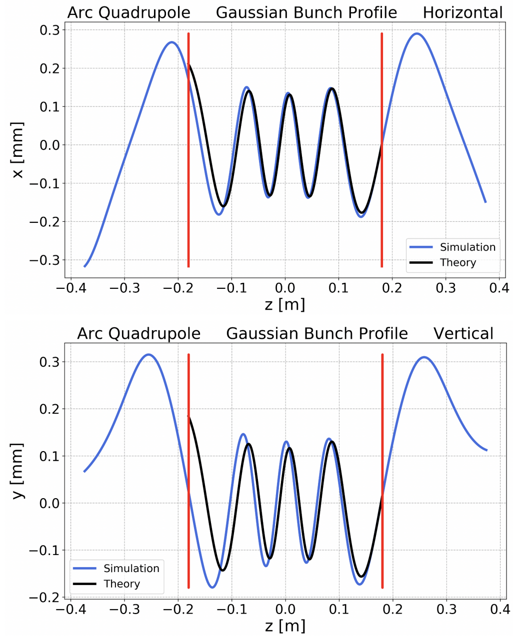

Figure 4: Comparison between macro-particle simulations and the linear theory of the electron trajectories within a Gaussian bunch in an LHC arc quadrupole [16].

This is due to the large range of the time and distance scales involved in the process. The entire chamber must be simulated and, at the same time, the small beam must be resolved very well, requiring a fine grid mesh over a large area. The fast electron motion requires small time steps, of the order of 10 ps, but the instability evolution can take several seconds amounting to a very large number of time steps. Consequently, electron cloud simulations can benefit from advanced computational methods such as multi-grid Poisson solvers and parallel computing [25,26]. However, due to the sequential nature of the electron cloud build-up, parallelization strategies are more limited than e.g. for simulations with only a lumped impedance. Even with advanced techniques, a single simulation can require several weeks of computing time on tens or hundreds of CPU cores.

MITIGATION STRATEGIES

Electron and ion instabilities can naturally be mitigated by preventing the accumulation of the corresponding particles. One approach to achieving this is to directly suppress the production of electrons and ions. A first step towards suppressing primary electrons and ions is to ensure a good vacuum or low residual gas pressure, to which end chamber surfaces with low outgassing or active pumping such as Non Evaporable Getter (NEG) coatings can be helpful [27]. For ion instabilities, this can be a sufficient measure to prevent significant accumulation. For electron cloud prevention, it may be necessary to suppress also the amount of photoelectrons emitted by the synchrotron radiation e.g. with the help of saw-tooth surfaces [28]. Furthermore, it is not sufficient to suppress primary electron production if secondary emission is large, as this can lead to exponential growth of the electron density.

Secondary electron emission can be suppressed through several different methods. For many materials, conditioning the surface with electrons lowers the secondary emission yield as a function of the accumulated electron dose [29]. This allows for beam-induced conditioning (or scrubbing), occurring gradually during accelerator operation [30]. Another commonly used technique is to coat exposed surfaces with materials that naturally have a low SEY, such as amorphous carbon or NEG [31,32]. In addition, a low SEY can also be achieved by modifying the surface topology, e.g. through laser ablation [33,34].

An alternative, or complementary, approach to direct suppression is to actively perturb the electron and ion motion, so as to prevent their accumulation. This can be achieved e.g. by using clearing electrodes, which generate electric fields that attract the charged particles towards the walls [35–38]. For electrons, a similar effect can be achieved with weak magnetic fields that bend the trajectories of emitted particles back onto the chamber wall, such as solenoids [39,40].

If accumulation cannot be prevented, there are some means of addressing the resulting instabilities. Coupled-bunch instabilities, whether due to electrons or ions, can typically be suppressed with conventional bunch-by-bunch transverse feedback systems, see Fig. 5. Landau damping can also help mitigate coupled-bunch instabilities from electrons and ions. For ion instabilities, a spread in the ion oscillation frequencies e.g. due to the non-linearity of the beam field and the presence of different ion species can give rise to Landau damping that has a mitigating effect on the instability [2,42]. Amplitude detuning from octupole magnets can mitigate the coupled-bunch electron instability [43].

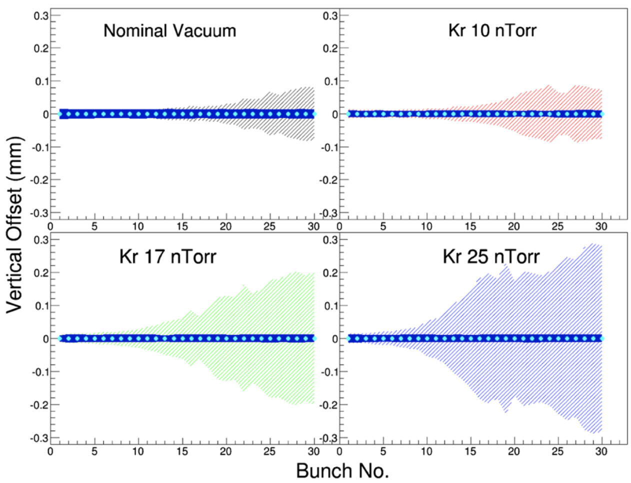

Figure 5: Vertical bunch offsets as a function of bunch number measured at CESR-TA with different Kr gas pressures [41]. With the transverse feedback switched on (filled area in blue) the fast beam-ion instability is fully suppressed.

Single-bunch electron instabilities, on the other hand, typically cannot be efficiently suppressed with conventional feedback systems, due to their characteristic fast intra-bunch motion. Wideband feedback systems, currently under development, have the potential to efficiently suppress also the fast intra-bunch motion [44]. Meanwhile, chromaticity and amplitude detuning from octupole magnets can suppress the instabilities to some extent [45].

Since both the electron and ion densities needed to cause instabilities accumulate over several bunch passages, the instabilities can also be mitigated by tailoring the filling pattern to minimize their accumulation. This can be achieved e.g. by increasing the bunch spacing or reducing the length of bunch trains [8,41,46], although it often comes at the cost of a reduced total beam current.

ELECTRON-ION INSTABILITIES

Above, it has been assumed that any seed particles with the same sign of electrical charge as the beam are negligible as they don't accumulate in the chamber volume, since they are repelled by the beam and eventually will reach the chamber walls and be absorbed. In this section, we discuss conditions under which this may not be a reasonable assumption.

Certainly, in most situations some effects that impact the dynamics indirectly can occur at the wall, such as outgassing when repelled ions or electrons impact on the wall. Apart from such potential secondary effects, it is reasonable to ignore the second species when the amount of seed particles produced at each bunch passage is small compared to the accumulated charge in the electron or ion cloud. On the other hand, if large amounts of electrons and ions are generated at each bunch passage, e.g. if very high gas densities occur in the beam pipe, one can expect the two species to have a significant impact on each other's dynamics. This could result in a collective behaviour involving the two species that is qualitatively different from the behaviour of either species on its own.

Events falling under this category occurred in the LHC during operation in 2017 and 2018 [47]. The recurring events, which were characterized by very fast beam instabilities accompanied by unusual beam losses in a certain machine location, would inevitably lead to beam dumps. The instabilities are thought to have been caused by a very high local gas density, predicted by beam loss rates to 10^{18}–10^{22} m^{-3}, depending on the longitudinal extent of the gas [48]. These transient pressure bumps were generated by the beam-induced phase transition of macro-particles of frozen air, present due to an accidental inlet of air during the preceding machine cool-down.

Observations of large positive tune shifts and fast intra-bunch motion suggest that large electron densities were present during the events [49]. However, electron cloud simulations with high gas densities could not reproduce the observations [50]. To model the instability, electron cloud simulation tools were extended with multi-cloud capabilities to model both the build-up and beam stability in the presence of electrons and ions simultaneously [51]. For high gas densities, the simulations show a significant impact of the

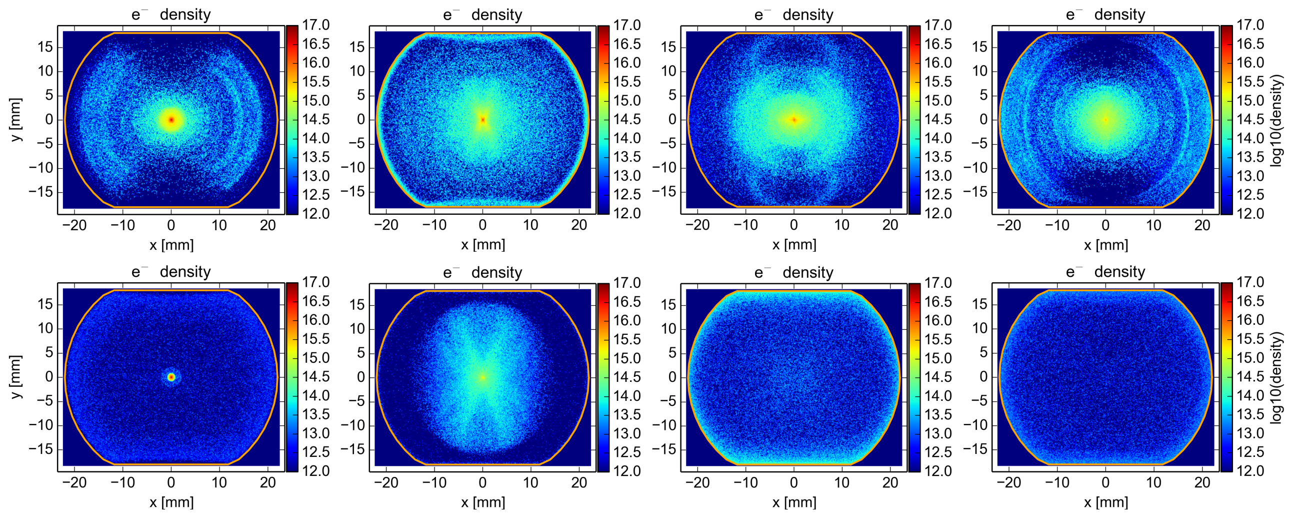

(a) t = 0 (b) t = 1 ns (c) t = 5 ns (d) t = 15 ns

Figure 6: Simulation snapshots of the electron density in the LHC beam chamber during a bunch passage [51]. Images from a multi-species simulation (top), are compared to the equivalent images in a simulation tracking only electrons (bottom). The first image on each row (t = 0) is taken during the passage of the centre of the bunch.

field from the ion population on the electron dynamics, as illustrated in Fig. 6, confirming that, at high concentrations, the two species must be modelled together.

OUTLOOK

Electron and ion instabilities have been observed in several machines. Electron cloud is present in several operating machines. Ion instabilities are currently observed mainly under vacuum degradation, but may become more prevalent in future machines with higher beam brightness. In addition, an instability mechanism relying on the interplay between electrons and ions may occur under exceptional conditions.

In order to avoid problems from electron and ion instabilities, predictions and development of mitigation strategies are important. Macro-particle simulations can model the phenomena comprehensively using modern computational tools, but large amounts of computing time and resources are still needed for realistic simulations. For electron cloud, the development and implementation of mitigation strategies are needed for several on-going as well as future projects, such as the HL-LHC and the FCC. For ion instabilities more comprehensive studies are needed to assess their impact in future machines.

ACKNOWLEDGEMENTS

The author would like to thank G. Arduini, G. Iadarola, E. Métral, A. Oeftiger, A. Romano, G. Rumolo, and L. Sabato for their input to the present contribution.

REFERENCES

[1] T. O. Raubenheimer and F. Zimmermann, "Fast beam-ion instability. I. Linear theory and simulations", *Phys. Rev. E* 52, pp. 5487–5498, 1995.

[2] G. V. Stupakov, T. O. Raubenheimer, and F. Zimmermann, "Fast beam ion instability. 2. Effect of ion decoherence", *Phys. Rev. E* 52, pp. 5499–5504, 1996.

[3] F. Zimmermann and G. Rumolo, "Two stream problems in accelerators", proceedings of APAC'01, Beijing, China, 2001.

[4] F. Zimmermann, "Two-stream effects in present and future accelerators", proceedings of EPAC2002, Paris, France, 2002.

[5] M. Bassetti and G. Erskine, "Closed expression for the electrical field of a two-dimensional Gaussian charge", Technical Report, CERN-ISR-TH/80-06, 1980.

[6] S. Heifets, "Saturation of the ion transverse instability", proceedings of PAC'97, Vancouver, Canada, 1997.

[7] L. Mether, A. Oeftiger, and G. Rumolo, "Modeling of fast beam-ion instabilities", *CERN Yellow Rep. Conf. Proc.* 1, pp. 63–68, 2018.

[8] L. Wang, Y. Cai, T. O. Raubenheimer, and H. Fukuma, "Suppression of beam-ion instability in electron rings with multi-bunch train beam fillings", *Phys. Rev. ST Accel. Beams* 14, p. 084401, 2011.

[9] L. Wang *et al*, "Beam ion instability: Measurement, analysis, and simulation", *Phys. Rev. ST Accel. Beams* 16, p. 104402, 2013.

[10] G. Iadarola and G. Rumolo, "Electron cloud effects", *CERN Yellow Rep. Conf. Proc.* 1, pp. 49–56, 2018.

[11] G. Iadarola *et al.* "Electron cloud studies for the upgrade of the CERN PS", proceedings of IPAC'13, Shanghai, China, 2013, paper WEPEA013.

[12] F. Zimmermann, "Electron-cloud effects in past and future machines – walk through 50 years of electron-cloud studies", proceedings of ECLOUD'12, Isola d'Elba, Italy, 2012.

[13] J. F. Esteban Müller, P. Baudrenghien, T. Mastoridis, E. Shaposhnikova, and D. Valuch, "High-accuracy diagnostic tool for electron cloud observation in the LHC based on synchronous phase measurements", *Phys. Rev. ST Accel. Beams* 18, p. 112801, 2015.

[14] G. Rumolo *et al*, "Electron cloud effects at the LHC and LHC injectors", proceedings of IPAC'17, Copenhagen, Denmark, 2017, paper MOZA1.

[15] K. Ohmi, "Coherent and incoherent effects of e-cloud", presented at MCBI 2019, this conference.

[16] L. Sabato, "Analysis of electron motion within the beam", presentation at the 65th Electron Cloud Meeting, CERN, Feb. 2019. `https://indico.cern.ch/event/790352/`

[17] K. Ohmi and F. Zimmermann "Head-tail instability caused by electron clouds in positron storage rings", *Phys. Rev. Lett.* 85, pp. 3821–3824, 2000.

[18] K. Ohmi, F. Zimmermann, and E. Perevedentsev, "Wake-field and fast head-tail instability caused by an electron cloud", *Phys. Rev. E* 65, p. 016502, 2002.

[19] E. Perevedentsev, "Head-tail instability caused by electron cloud", proceedings of ECLOUD'02, Geneva, Switzerland, 2002.

[20] G. Rumolo and F. Zimmermann, "Electron cloud simulations: beam instabilities and wakefields", *Phys. Rev. ST Accel. Beams* 5, p. 121002, 2002.

[21] G. Iadarola, "New tools for the simulation of coupled bunch instabilities driven by electron cloud", presentation at the 64th Electron Cloud Meeting, CERN, Dec. 2018. `https://indico.cern.ch/event/776089/`

[22] G. Arduini *et al.*, "Beam observations with electron cloud in the CERN PS and SPS complex", proceedings of ECLOUD'04, Napa, USA, Apr. 2004.

[23] S. S. Win *et al.*, "Numerical study of coupled-bunch instability caused by an electron cloud", *Phys. Rev. ST Accel. Beams* 8, p. 094401, 2005.

[24] S. A. Antipov, P. Adamson, A. Burov, S. Nagaitsev, and M.-J. Yang, "Fast instability caused by electron cloud in combined function magnets", *Phys. Rev. Accel. Beams* 20, p. 044401, 2017.

[25] J.-L. Vay, M. A. Furman, and M. Venturini, "Direct numerical modeling of e-cloud driven instability of three consecutive batches in the CERN SPS", proceedings of IPAC'12, New Orleans, Louisiana, USA, 2012, paper TUEPPB006.

[26] G. Iadarola *et al.*, "Evolution of Python tools for the simulation of electron cloud effects", proceedings of IPAC'17, Copenhagen, Denmark, 2017, paper THPAB043.

[27] C. Benvenuti *et al.*, "A novel route to extreme vacua: the non-evaporable getter thin film coatings", *Vacuum* 53, pp. 219–225, 1999.

[28] N. Mahne *et al.*, "Photon reflectivity distributions from the LHC beam screen and their implications on the arc beam vacuum system", *Appl. Surf. Sci.* 235, pp. 221–226, 2004.

[29] R. Cimino *et al.*, "Nature of the decrease of the secondary-electron yield by electron bombardment and its energy dependence", *Phys. Rev. Lett.* 109, p. 064801, 2012.

[30] G. Iadarola, B. Bradu, P. Dijkstal, L. Mether, and G. Rumolo, "Impact and Mitigation of Electron Cloud Effects in the Operation of the Large Hadron Collider", proceedings of IPAC'17, Copenhagen, Denmark, 2017, paper TUPVA019.

[31] C. Yin Vallgren *et al.*, "Amorphous carbon coatings for the mitigation of electron cloud in the cern super proton synchrotron", *Phys. Rev. ST Accel. Beams*, vol. 14, p. 071001, 2011.

[32] B. Henrist, N. Hilleret, C. Scheuerlein, and M. Taborelli, "The secondary electron yield of TiZr and TiZrV non-evaporable getter thin film coatings", *Appl. Surf. Sci.* 172, pp. 95–102, 2001.

[33] G. Tang, A. C. Hourd, and A. Abdolvand, "Nanosecond pulsed laser blackening of copper", *Appl. Phys. Lett.* 101, p. 231902, 2012.

[34] O. B. Malyshev *et al.* "Electron cloud effect mitigation with the laser ablation technique", presented at MCBI 2019, this conference.

[35] F. Caspers, JP. Delahaye, JC. Godot, K. Hubner, and A. Poncet, "EPA beam-vacuum interaction and ion clearing system", proceedings of EPAC'88, Rome, Italy, 1988.

[36] M. Zobov *et al.*, "Impact of Ion Clearing Electrodes on beam dynamics in DAΦNE", *J. Instrum.* 2, p. 08002, 2007.

[37] L. F. Wang, D. Raparia, J. Wei, and S.Y. Zhang, "Mechanism of electron cloud clearing in the accumulator ring of the Spallation Neutron Source", *Phys. Rev. ST Accel. Beams* 7, p. 034401, 2004.

[38] Y. Suetsugu *et al.*, "Demonstration of electron clearing effect by means of a clearing electrode in high-intensity positron ring", *Nucl. Instrum. Meth. A* 598, pp. 372–378, 2009.

[39] H. Fukuma *et al.*, "Status of solenoid system to suppress the electron cloud effects at the KEKB", *AIP Conf. Proc.* 642, pp. 357–359, 2002.

[40] A. Kulikov, A. Novokhatski, and J. Seeman, "Suppression of the beam instability related to electron cloud at PEP-II B-factory", proceedings of ECLOUD'04, Napa, CA, USA, 2004, pp. 21-24.

[41] A. Chatterjee, K. Blaser, W. Hartung, D. Rubin, and S. T. Wang, "Fast ion instability at the Cornell Electron Storage Ring Test Accelerator", *Phys. Rev. ST Accel. Beams* 18, 064402, 2015.

[42] G. Stupakov, "Suppression of the fast beam-ion instability by tune spread in the electron beam due to beam-beam effects", presented at MCBI 2019, this conference.

[43] L. Mether, "Electron cloud stability at injection: coupled bunch effects", presented at the 165th HL-LHC WP2 meeting, CERN, Dec. 2019. `https://indico.cern.ch/event/863723/`

[44] K. Li *et al.*, "Modelling and studies for a wideband feedback system for mitigation of transverse single bunch instabilities", proceedings of IPAC'13, Shanghai, China, 2013, p. 3019.

[45] K. Li and G. Rumolo, "Mitigation of electron cloud instabilities in the LHC using sextupoles and octupoles", proceedings of IPAC'12, New Orleans, LA, USA, 2012, p. 3084.

[46] G. Skripka *et al.* "Comparison of electron cloud build-up simulations against heat load measurements for the LHC arcs with different beam configurations", proceedings of IPAC'19, Melbourne, Australia, 2019, paper WEPTS051.

[47] J. M. Jiménez *et al.*, "Observations, analysis and mitigation of recurrent LHC beam dumps caused by fast losses in arc half-cell 16L2", proceedings of IPAC'18, Vancouver, Canada, 2018, paper MOPMF053.

[48] A. Lechner *et al.*, "Beam loss measurements for recurring fast loss events during 2017 LHC operation possibly caused by macroparticles", proceedings of IPAC'18, Vancouver, Canada, 2018, paper TUPAF040.

[49] B. Salvant *et al.*, “Experimental characterisation of a fast instability linked to losses in the 16L2 cryogenic half-cell in the CERN LHC”, proceedings of IPAC’18, Vancouver, Canada, 2018, paper THPAF058.

[50] L. Mether *et al.*, “16L2: operation, observations and physics aspects”, proceedings of 7th Evian Workshop on LHC Beam Operation, Evian Les Bains, France, 2017, pp. 99–105.

[51] L. Mether, G. Iadarola, K. Poland, G. Rumolo, and G. Skripka, “Multi-species electron-ion simulations and their application to the LHC”, proceedings of IPAC’19, Melbourne, Australia, 2019, paper WEPTS050.